Final Report DOE Award No. DE-FG02-08ER46536

Northwestern University

Project Title: Materials Science of Electrodes and Interfaces for High-Performance Organic Photovoltaics

PIs: Tobin J. Marks (lead), Robert P. H. Chang, Arthur J. Freeman, Thomas O. Mason, Kenneth R. Poeppelmeier

Project Period: September 1, 2008 – December 31, 2014

Abstract

The science of organic photovoltaic (OPV) cells has made dramatic advances over the past three years with power conversion efficiencies (PCEs) now reaching ~12%. The upper PCE limit of light-to-electrical power conversion for single-junction OPVs as predicted by theory is ~23%. With further basic research, the vision of such devices, composed of non-toxic, earth-abundant, readily easily processed materials replacing/supplementing current-generation inorganic solar cells may become a reality. Organic cells offer potentially low-cost, roll-to-roll manufacturable, and durable solar power for diverse in-door and out-door applications. Importantly, further gains in efficiency and durability, to that competitive with inorganic PVs, will require fundamental, understanding-based advances in transparent electrode and interfacial materials science and engineering. This team-science research effort brought together an experienced and highly collaborative interdisciplinary group with expertise in hard and soft matter materials chemistry, materials electronic structure theory, solar cell fabrication and characterization, microstructure characterization, and low temperature materials processing. We addressed in unconventional ways critical electrode-interfacial issues underlying OPV performance -- controlling band offsets between transparent electrodes and organic active-materials, addressing current loss/leakage phenomena at interfaces, and new techniques in cost-effective low temperature and large area cell fabrication. The research foci were: 1) Theory-guided design and synthesis of advanced crystalline and amorphous transparent conducting oxide (TCO) layers which test our basic understanding of TCO structure-transport property relationships, and have high conductivity, transparency, and tunable work functions but without (or minimizing) the dependence on indium. 2) Development of theory-based understanding of optimum configurations for the interfaces between oxide electrodes/interfacial layers and OPV active layer organic molecules/polymers. 3) Exploration and perfection of new processing strategies and cell architectures for the next-generation, large-area flexible OPVs. The goal has been to develop for the solar energy community the fundamental scientific understanding needed to design, fabricate, prototype, and ultimately test high-efficiency cells incorporating these new concepts. We achieved success in all of these directions.

Project Rationale

The past years have witnessed impressive advances in non-traditional solar cell science along with single-junction cell power conversion efficiencies (PCE) surpassing the half-way point to the maximum predicted by theory. The success of these record-breaking results comes from better understanding of the bulk and interfacial materials science, chemistry, and physics. In addition to synthesis and characterization, high-level predictive modeling and computation can help optimize the design parameters for new materials essential for high-performance devices. Especially challenging to the community is to develop models that explain the behavior at interfacial junctions and their connections to solar cell performance. The unique research

activities of this team fall within the center of a triangle whose three vertices are solid-state chemistry, high-level theory/modeling, and device fabrication and characterization. This coupled research mode has accelerated the understanding of the underlying science, which in turn has led to higher efficiency solar cell designs. The team has made important contributions to the energy conversion community, with important recent advances being: 1) Transparent conducting oxide (TCO) systems that rival ITO performance, but with significantly reduced In content; 2) TCO films grown at low temperature (hence compatible with flexible substrates) and having composite properties spanning amorphous and crystalline microstructures, yet with electrical performance near that of highly crystalline films; 3) Systematic, rational chemical surface/interface modifications that enhance charge extraction from the active layer, suppress interfacial recombination, and enhance electrode-active layer physical cohesion; 4) Demonstration of solar cell oxide interfacial layers with broadly tunable work functions to match active layer energy levels; 5) Mechanically flexible organic solar cells fabricated on plastic substrates and enabled by amorphous, flexible TCO electrodes. These and other significant experimental results have benefited greatly from the team's complementary theory and modeling activities.

Results and Accomplishments Y 1.

In the following section we report on the recent progress made in addressing parts 1 and 3 of our technical approach. Specifically, we will comment on efforts made to replace the currently preferred transparent anode, ITO, with alternative TCOs and to design interlayers that block incorrect charge from reaching the "wrong" electrode (e.g., electrons reaching the anode) or excitons from being quenched at electrodes.

Alternative TCOs

N-Type

As described in our proposal, owing to both chemical and electrical incompatibility, indium tin oxide (ITO) is not an ideal n-type electrode for OPVs. Furthermore, indium is relatively scarce and therefore costly. For these reasons, we are conducting an extensive investigation of ITO alternatives, such as ZITO (Zn-In-Sn-O), which contain much lower indium contents. Recently an important correlation was made between surface electronic behavior (Fermi level, work function) and the bulk defect structure of bixbyite-based ZITO materials. First of all, it was conclusively established in bulk specimens that the same Frank-Köstlin (F-K) associate $(2Sn_{In}^{\bullet}O_i'')^x$, which dominates the defect structure of ITO, also dominates the defect structure of Zn- and Sn-codoped In_2O_3. Second, thin films of nearly identical composition were deposited by rf-magnetron sputtering. The Fermi levels could be varied during deposition over a wide range (2.3-3.0 eV), which was attributed to changes of the bulk Fermi level (and changes in the F-K associate content). More importantly, the ionization potential of these films are increased by as much as 1 eV with a post-deposition oxygen anneal at intermediate temperatures (400-500^{o}C), with work functions of degenerately-doped (highly conductive) films reaching the 4-7-4.8 eV range. Our ability to tune the work function of ZITO will be incredibly important when actually building devices and we want to optimize energy level matching between the ZITO anode and the highest occupied molecular orbital of the organic photoactive layer.

In addition to ZITO, we are exploring In-doped CdO/Sn-doped In_2O_3 (CIO/ITO) bilayers as anode materials. These films are prepared by depositing thin ITO films by ion-assisted deposition (IAD) on CIO films grown by metal-organic chemical vapor deposition (MOCVD).

With a significantly lower In content (19 vs. ~93 at. %) and a greater conductivity/transparency figure of merit (0.049 vs. 0.043 Ω^{-1}) than commercial ITO films, these bilayer films are used as anodes in bulk-heterojunction (BHJ) organic photovoltaic (OPV) devices having a poly(2-methoxy-5-(3,7-dimethyloctyloxy)-1,4-phenylenevinylene (MDMO-PPV) + [6,6]-phenyl C_{61} butyric acid methyl ester (PCBM) active layer. This highly conductive bilayer anode can replace ITO in small, laboratory-sized cells and should significantly outperform ITO in larger-area cells.

The development of high-efficiency p-type transparent electrodes would allow for increased flexibility in OPV design and enable tandem solar cell operation. To this end we have been pursuing both crystalline and amorphous p-type TCOs. Recently, Rh^{3+}-based materials have attracted substantial interest as p-type TCOs (H. Mizoguchi *et al.*, *Appl. Phys. Lett.*, **2002**, *80*, 1207; M. Dekkers *et al.*, *Appl. Phys. Lett.*, **2007**, *90*, 021903). We have begun a joint theoretical/experimental study of crystalline $ZnRh_2O_4$ as an essential step toward understanding the behavior of amorphous materials.

Crystalline $ZnRh_2O_4$ was successfully synthesized by means of solid state reaction and was characterized for its electrical and optical properties. Analysis of the high temperature electrical properties of $ZnRh_2O_4$ indicated an activated mobility (activation energy ~0.25 eV), indicative of small polaron conduction. Four-point conductivity and thermopower measurements were carried out in air at elevated temperatures (650-800 °C). Carrier concentrations were on the order of 10^{21} cm^{-3}, with conductivities as high as 25 S/cm at 800°C. The bandgap of $ZnRh_2O_4$ was determined to be 2.2 eV by diffuse reflectance measurements.

Additionally, we are developing a novel hydrothermal method for the synthesis of TCOs. The focus of this work is to take model p-type TCO systems, such as delafossites and oxide chalcogenides, to gain insight into how the aqueous behavior of metal cations and anions effects product formation. Through this we hope to be able to consider any metal cation/anion combination and *a priori* rationally determine the conditions necessary for phase formation. One model system we have considered is BiCuOQ (Q=S, Se), which is isostructural to the layered *p*-type transparent conductor LaCuOS. BiCuOSe and BiCuOS were prepared by a hydrothermal reaction of Bi_2O_3, Cu_2O, Se (or Na_2S), and hydrazine (only BiCuOSe) at a lower reaction temperature (250 °C) and time (48 h) than in previously reported solid state syntheses. A subtle balance between the solubilization of Bi_2O_3 and Cu_2O and the stabilization of monovalent copper and dianionic selenium/sulfur was achieved by the selection of a reaction temperature of 250 °C. The measured conductivity of hydrothermally prepared BiCuOSe samples ($\sigma \approx 3.3$ S cm^{-1}) is greater than values reported for non – doped LnCuOS (Ln = La, Pr, Nd) and LaCuOSe samples and compares well with those of BiCuOS (0.08(2) S cm^{-1}), CeAgOS, and CeCuOS. Owing to scalar relativistic effects associated with the large bismuth cations, the band gaps are reduced (BiCuOSe: E_g = 0.75 eV; BiCuOS: E_g = 1.09 eV), limiting their utility as *p*-type transparent conductors.

Charge Blocking Interlayers

Organic Interlayers

With respect to organic interfacial layers, an investigation of anode/active layer interface modification in bulk-heterojunction organic photovoltaics (OPVs) is carried out using poly(3,4-ethylenedioxythiophene):poly(styrene sulfonate) (PEDOT:PSS) and/or a hole transporting/electron-blocking blend of 4,4'-bis[(*p*-trichlorosilylpropylphenyl)-

phenylamino]biphenyl ($TPDSi_2$) and poly[9,9-dioctylfluorene-*co*-N-[4-(3-methylpropyl)]-diphenylamine] (TFB). Current–voltage scans in AM1.5G light and dark and impedance spectroscopy in the dark show the $TPDSi_2$:TFB blend produces MDMO-PPV:PCBM OPVs with increased open-circuit voltage (V_{oc}), power conversion efficiency, thermal stability, and mean charge carrier lifetime compared to devices with no interfacial layer (IFL) or with PEDOT:PSS. Using PEDOT:PSS and $TPDSi_2$:TFB together in the same cell greatly reduces dark current, further increases carrier lifetime, and produces the highest V_{oc} (0.91 V) by combining the electron-blocking effects of both layers. Also, ITO anode pre-treatment was investigated by X-ray photoelectron spectroscopy to understand why oxygen plasma, UV ozone, and solvent cleaning markedly affect cell response in combination with each IFL. The O_2 plasma and UV ozone treatment (30 min) most effectively clean the ITO surface and are the best methods to prepare the surface for PEDOT:PSS deposition; UV ozone (5 min) produces optimum solar cells fabricated with a $TPDSi_2$:TFB IFL; and solvent cleaning leaves significant residual carbon contamination on the ITO and is best followed by an additional O_2 plasma or UV ozone treatment. This work was then extended to conjugated anthrancene derivatives as active layers.

Inorganic Interlayers

In addition to organic electron-blocking layers, we have also been studying the effectiveness of various inorganic p-type TCOs. Experimentally, NiO deposition on ITO (indium tin oxide) for OLED applications has been shown to increase the work function of ITO (~4.8 eV) dramatically to 5.4 eV, which is closer to the optimum level of the HOMO (highest occupied molecular orbital) in the organic layer of OLEDs. Owing to the better energy level matching between the NiO Fermi level (~ 5.0 eV) and the HOMO of the organic layer and the high CBM of NiO (~1.8eV), the insertion of NiO thin layers between the organic photoactive layer and the ITO anode of BHJ solar cells has shown an increase to 5.2% power conversion efficiency (5.6% confirmed by NREL).

To better understand the role of NiO as an electron blocking layer, work functions and effective masses of NiO were calculated theoretically using the full potential linearized augmented plane wave (FLAPW) method. The calculations were performed within the local spin density approximation (LSDA) (L. Hedin and B. I. Lundqvist, *J. Phys. C*, **1971**, *4*, 2064) and the LSDA+U method (A. B. Shick *et al.*, *Phys. Rev. B*, **1999**, *60*, 10763) was employed to treat the highly correlated Ni 3*d* electrons and to compare with the LSDA results.

Compared to the NiO bulk band gap, the band gaps of NiO films are significantly reduced due to the surface states near the VBM and CBM. The band gaps with the LSDA+U method are 3.4, 2.9, 1.2, 1.7 eV for NiO bulk, NiO (001) films, Ni terminated, and O terminated NiO (111) films, respectively, which are significantly enlarged compared to the LSDA band gaps, 0.4 and 0.01 eV for NiO bulk and NiO (001) films, respectively.

The work function for the non-polar (001) surface of the 9-layer NiO film is predicted to be approximately 4.71 eV within the LSDA, which is calculated from the valence band maximum. It is known that NiO is always a p-type semiconductor due to intrinsic metal vacancies (S. Hüfner, *Adv. Phys.*, **1994**, *43*, 183). However, the LSDA+U calculations yield a significantly larger work function value, 5.78 eV. For the polar NiO (111) surfaces, it has been known that strong surface reconstructions, such as octopolar (p(2x2)) surface structures, are required due to the instability of polar surfaces (W.-B. Zhang, B.-Y. Tang, *J. Chem. Phys.*, **2008**, *128*, 124703). We thus created most stable Ni and O terminated octopolar surface structures using a symmetric

NiO with 11 layers in the [111] orientation, and optimized the geometry fully. The calculated work functions with the LSDA+U method are 5.44 and 6.83 eV for the Ni and O polar surfaces, respectively. Compared to the LSDA results, these values are also higher by 0.5 and 1.1 eV for Ni and O terminated surfaces, respectively. From the LSDA+U results, the polycrystalline NiO films are expected to have about 6.0 eV for the work function.

Results and Accomplishments Y2, 3

In the following section we report on our Years 2,3 progress, moving from bulk synthesis, to thin films, to theoretical studies, and finally to PV cell studies.

Bulk Synthesis and Studies of Transparent Electrode Materials

P-Type Transparent Conductors

The development of a p-type transparent conductor with conductivity comparable to the best n-type TCOs would be a major advance. In the last reporting period we outlined a synthetic strategy for the hydrothermal synthesis of novel p-type transparent conductors. BiCuOSe and BiCuOS were prepared by a hydrothermal reaction of Bi2O3, Cu2O, Se (or Na2S), and hydrazine (only BiCuOSe) at a lower reaction temperature (250oC) and time (48 h) than in previously reported solid state syntheses. A subtle balance between the solubilization of Bi2O3 and Cu2O and the stabilization of monovalent copper and dianionic selenium/sulfur was achieved by the selection of a reaction temperature of 250oC. Through the selection of the appropriate temperature and pH, we have adapted this approach towards the synthesis of a number of new materials, and TCO testing (electrical, optical) is underway.

Regardless of our insights into the reaction mechanisms, reaction rates are inherently limited by the heating method. In a typical hydrothermal reaction an oven is heated to a certain temperature, which heats the pressure vessel, which in turn heats the aqueous solution and initiates the reaction. Potential drawbacks of this method include slow heating as well an inverse temperature gradient with the solution near the wall of the vessel being warmer than the inner core. This can be overcome through the use of microwave-hydrothermal technology. The experimental setup is very similar to that of generic hydrothermal reactions, but microwaves are used to locally heat the water, which leads to more uniform heating. Microwave-hydrothermal methods have demonstrated improved reaction kinetics and therefore faster reaction times and uniform product morphology are observed. Microwave-hydrothermal technology has also been utilized to prepare new phases that are unobtainable by conventional hydrothermal methods. We have therefore implemented a microwave-hydrothermal synthesis system and will apply the knowledge gained concerning metal cation speciation and solubility and their effect on product formation in this microwave-hydrothermal system. We anticipate the discovery of new phases, enhanced doping capabilities, and an extension from bulk synthesis to solution-deposited thin films.

N-Type Transparent Conductors

Owing to both chemical and electrical incompatibility issues with other OPV components, indium tin oxide (ITO) is not the “ideal” n-type electrode for organic photovoltaics. Furthermore, indium is relatively scarce such that its cost is highly volatile. For these reasons, we are conducting an extensive investigation of ITO alternatives, such as ZITO

(Zn-In-Sn-O) [Harvey, et al., 2009], which contain much lower indium contents. Recently, Extended X-ray Absorption Fine Structure (EXAFS) investigations were performed on both crystalline and amorphous ZITO thin films. EXAFS results confirmed that Zn and Sn are substitutional dopants, and suggest that an oxygen rearrangement occurs that leads to a higher oxygen coordination around the Sn atoms and lower coordination around the Zn [Proffit, et al., 2009]. The excess Sn-coordination is consistent with the well-established Frank-Köstlin associates (Sn- donors and oxygen interstitial acceptors) in ITO and related materials (e.g., ZITO).

To increase the efficiency of an organic photovoltaic cell, it is crucial to optimize the energy level (i.e., work function and ionization potential) match between the TCO anode and the highest occupied molecular orbital (HOMO) of the organic photoactive layer. For a given material, a range of work function and ionization potential is available, depending on film deposition conditions and post-deposition treatments. X-ray Photoelectron Spectroscopy (XPS) and Ultraviolet Photoelectron Spectroscopy (UPS) experiments were performed at the Technical University of Darmstadt to measure the available ranges of work function and ionization potential for three technologically important TCO systems: ZnO:Al, SnO_2:Sb, and In_2O_3:Sn,Zn [Klein, *et al.*, 2009]. The work functions varied from 3.5 – 5.2 eV for ZnO, 4.4 – 5.7 eV for pure SnO_2, 4.1 – 5.6 eV for SnO_2:Sb, and 4.0 – 5.5 eV for In_2O_3, ITO, and ZITO films. The ionization potential could be varied over a range of approximately 1 eV for each system by changing crystallographic orientation during deposition (ZnO) or surface dipoles during post- deposition oxidation (SnO_2, In_2O_3). Further investigation into the factors governing changes in work function and ionization potential of transparent electrodes could lead to an enhanced ability to tailor material properties and thereby increase device efficiency.

We are currently investigating the defect chemistry of the $In_2O_3(ZnO)_k$ (k = integer) homologous series of compounds. These phases are attractive as TCOs because they have less than 50% indium on a cation basis, but maintain conductivities comparable to ITO. Aliovalent doping is relatively ineffective at increasing the carrier content, so a better understanding of the defect chemistry in this system is necessary to better control its properties. The work involves a close collaboration between physical property measurements (electrical, optical) and first principles theory efforts (see below).

Thin Film Transparent Electrode Studies

Building on our success with the development of crystalline ZITO (Zn-In-Sn-O) as a lower cost alternative to ITO (In-Sn-O) we extended our research to the investigation of disordered/amorphous ZITO (a-ZITO) thin film TCOs. These materials can be grown by pulsed laser deposition (PLD) at room-temperature, making it compatible with substrates, such as plastics, that cannot tolerate the higher growth-temperatures needed for crystalline materials. It was found that by tailoring the oxygen partial-pressure during film growth, disordered a-ZITO films as transparent as their crystalline counterparts could be grown at room-temperature while still maintaining high electrical-conductivity (~1500 S/cm) (Buchholz et al., 2009). These films were also found to be superior to their crystalline counterparts in flexibility; they maintain high electrical performance after repeated flexing.

Until recently, our work focused on 30% substitution of In by Sn/Zn (ZITO-30). Recently, however, we have significantly extended the cosubstitution level. In crystalline form, the solubility limit for cosubstitution is about 40%. We have been able to deposit a-ZITO well beyond this crystalline solubility limit, at both 50% substitution (ZITO-50) and even 70% substitution (ZITO-70) levels. Although the transparency of all the films remained high, the electrical conductivity was found to decrease somewhat as the fraction of cosubstitution increased, through a reduction of both carrier concentration and mobility. Ongoing work is addressing whether or not the electrical properties can be recovered by the choice of PLD growth parameters, while still maintaining high degrees of cosubstitution. The significance of this effort lies in the reduction of costly indium.

Theoretical Studies

In support of the experimental studies on $In_2O_3(ZnO)_k$, a series of TCOs that have electrical and optical properties rivaling In_2O_3, but with less than 50% of the indium content, we calculated the electronic structure properties of $In_2O_3(ZnO)_k$ (k=1, 2, 3) using both local density approximation (LDA) and screened-exchange LDA (sX-LDA). The LDA/sX-LDA band gaps are 0.811/3.060, 0.636/2.642 and 0.877/3.036eV for the k = 1, 2, 3 phases, respectively. The sX-LDA band gaps are in good agreement with experimental data (k = 3). The k = 1 phase has an indirect band gap which is 0.129/0.108eV (LDA/sX-LDA) smaller than the direct band gap at the *Brillouin* zone center. For all three phases, near the band edge, the conduction bands are much more dispersive than the valence bands. For the odd k phases, the top valence bands are very flat in all three reciprocal lattice vector directions. For the k=2 phase, however, we found strong anisotropic characteristics. There are largely dispersive bands in the *xy* plane, which is not the case in the other two odd k phases, while in the *z* direction the top valence bands are flat in such a way that they are totally separated from the rest of the valence bands. These characteristics can be attributed to the pure ZnO layers which only exist in the k=2 phase. The site-projected density of states show that these states are mostly contributed by the Zn-*d* and O-*p* shells of the atoms in these pure ZnO layers. This work is helping us to interpret the physical properties (experimental data) being measured on these k-phase materials.

Interestingly, the k-phase materials are candidates for both TCO and thermoelectric energy-conversion applications. To investigate theoretically the transport properties such as Seebeck coefficients (α) and the electrical conductivities (σ) and to understand their relationship with the electronic structures, we employed the Boltzmann distribution function in the constant relaxation time approximation. The constant relaxation time was found by fitting the calculated results to the experimental data point ($\alpha \sim -438$ □V/K and $\sigma \sim 11.49$ S/cm), which is 10-14 s. To determine the group velocities which are used in the transport coefficients, we use full intraband optical matrix elements calculated within the FLAPW method. Different carrier concentrations for the transport coefficient calculations were treated within the rigid band model, and the Fermi-Dirac distribution function at 1025 K was used for the temperature contribution.

It was found that the theoretical calculations show nearly identical Seebeck coefficients and conductivities between different k-phases (k=1, 2, and 3) for any given carrier concentrations. As the conductivity increases due to the higher carrier concentration/chemical potential, the Seebeck coefficient decreases, which is typical behavior. According to the Jonker analysis, the ratio between α and $\ln\sigma$ (i.e. $\alpha/\ln\sigma$) should be k_B/e, which is 86.15 μV/K.

We found that the linear fit of all calculated data points yields approximately 76.7 μV/K, but using only the first two data points for the fitting yields the value of 84.48 μV/K, which is close to the ideal one. This discrepancy originates from the fact that the effective mass as a function of the carrier concentration (or chemical potential) is not a constant, which is not taken into account in the Jonker analysis. Indeed, we found that the change in the effective mass is larger as the carrier concentration increases.

As a p-type TCO candidate, we also performed the first-principles calculations of $ZnRh_2O_4$ to understand the electronic structure and conductivity. The results shows that compared to conventional TCO's whose band gaps form between O 2p states and the cation s or d states, $ZnRh_2O_4$ has a band gap determined by crystal splitting of the Rh *t2g* (fully occupied) and *eg* states (fully empty). The p-type conductivity of $ZnRh_2O_4$ is thought to be a consequence of the high lying VBM from Rh 4d with reduced defect compensation when compared with the low lying O 2p in other TCO materials with stronger defect compensation.

Photovoltaic Cell Studies

In studies to simplify the fabrication of bulk-heterojunction organic photovoltaic (OPV) devices, it was found that when glass/tin-doped indium oxide (ITO) substrates are treated with dilute aqueous HCl solutions, followed by UV-ozone (UVO), and then used to fabricate OPV devices of the structure glass/ITO/P3HT:PCBM/LiF/Al (P3HT = poly-3-hexylthiophene; PCBM = [6,6]- phenyl C_{61} butyric acid methyl ester), device performance is greatly enhanced. Light-to-power conversion efficiency (Eff) increases from 2.4% for control devices in which ITO surface is treated only with UVO, to 3.8% with the HCl + UVO treatment – effectively matching the performance of an identical device having a PEDOT:PSS (poly(3,4-ethylenedioxythiophene): poly(styrenesulfonate)) anode interfacial layer. The enhancement originates from increases in V_{OC} from 463 mV to 554 mV, and FF from 49% to 66%. The modified-ITO device also exhibits a 4x enhancement in thermal stability versus an identical device containing a PEDOT:PSS anode interfacial layer. To understand the origins of these effects, the ITO surface is being analyzed as a function of treatment by ultraviolet photoelectron spectroscopy work function measurements, X-ray photoelectron spectroscopic composition analysis, and atomic force microscopic topography and conductivity imaging.

In studies to increase OPV anode electrical conductivity, the high conductivity of In-doped CdO (CIO) was combined with the corrosion resistance of Sn-doped In_2O_3 (ITO). Thus, CIO/ITO double-layer transparent conducting oxide thin films were prepared by depositing thin ITO films by ion-assisted deposition (IAD) on CIO films grown by metal-organic chemical vapor deposition (MOCVD) on glass substrates. These double-layer films were used as anodes in bulk-heterojunction (BHJ) organic photovoltaic (OPV) devices having a poly(2-methoxy-5-(3,7-dimethyloctyloxy)-1,4-phenylenevinylene (MDMO-PPV) and [6,6]-phenyl C61 butyric acid methyl ester (PCBM) blend as the active layer. These double-layer films thus have an In content of only 19% and a slightly greater figure of merit (FOM, $\Phi = T10/R_{sheet}$) = 0.0486 Ω-1 than commercial ITO films (In ~93%; FOM ~0.0427 Ω-1). OPV power conversion efficiencies of 1.10% and 1.49% are achieved on CIO/ITO-based OPV devices having poly(3,4-ethylenedioxythiophene):poly(styrenesulfonate) (PEDOT:PSS) or 4,4'-bis[(p-trichlorosilyl-propylphenyl)-phenylamino]biphenyl:poly[9,9-dioctylfluorene-co-N-[4-(3-methylpropyl)]-diphenylamine] (TPDSi2:TFB), respectively, as interfacial layers—comparable to ITO-

based control devices. These results demonstrate that CIO/ITO double-layers are promising low-In content, highly conductive and transparent electrode candidates for large-area optoelectronic devices.

Research Accomplishments Y4-6

The research goals of this 5-PI effort are: 1.) Design (based on theory) and synthesis of advanced TCO layers with high conductivity and transparency but without (or minimizing) the use of indium. 2.) Development of a theory-based understanding of what is the best configuration for the ideal interface between oxide electrodes/interfacial layers and OPV organic active layers composed of molecules and polymers. 3.) Exploration and development of new processing techniques and cell architecture for the next generation of large-area flexible OPVs. It is our plan that results from our research will continue to lead the way and support other DOE-funded energy programs. During the first 16 months of our program, significant progress has been made in each of the above areas.

In a joint collaboration, the Mason and Freeman groups have investigated the TCO properties of the so-called "homologous series" of compounds in the In-Zn-O system, with the formulae, $In_2O_3(ZnO)_k$ (k being various integer values). By combined in situ high temperature "Brouwer analysis" (log-log plots of electrical properties vs. pO_2) and first principles calculation of defect formation energies, the majority defect species have been identified. Both approaches support anti-site defects (In on Zn sites) as the prevailing defect species. When compensated by zinc vacancies (shown by the Freeman group to have a comparably small formation energy as the anti-site defects), the pO_2-dependence of the electrons should be precisely -1/4, as observed experimentally in Brouwer analyses for the k=5,7,9 phases. In the case of the k=3 phase, the behavior is similar to that in Sn-doped In_2O_3 (ITO), with its characteristic -1/8 Brouwer slope, and suggest that similar defect complexes involving anti-site donors dominate the defect structure. This success of combined theory and experiment in determining the underlying defect structure(s) is the first of its kind for these important layered ITO-alternative compounds. These phases are significant owing to their significantly lower indium contents than ITO, e.g., 40% for k = 3.

In an international collaboration with A. Klein of the Technical University of Darmstadt, the surface electronic potentials of these same k-phases ($In_2O_3(ZnO)_k$, with k=2, 3, 5, 7, and 9) were studied by photoelectron spectroscopy in bulk and thin film form to determine their viability as TCO components in organic photovoltaic devices. It was found that on a work function vs. and Fermi level plot, all the k-phases fall on a line of constant ionization potential (7.7-7.8 eV), comparable to that of oxygen-stabilized In_2O_3 surfaces and oxygen-terminated polar and non-polar ZnO surfaces. More importantly, their surface potentials were relatively insensitive to post-fabrication treatments (i.e., pO_2, T changes). Their stability (and relatively high work functions) bodes well for application as robust transparent electrodes in photovoltaic applications. Furthermore, Kelvin probe measurements in ambient conditions (under which OPVs are usually fabricated) agree well with photoelectron spectroscopy measurements, yet another indication of their stability.

In a three-way collaboration between the Freeman, Mason and Poeppelmeier groups, TCO phases, including the scheelite ($Ga_{3-y}In_{5+y}Sn_2O_{16}$, where $0.2 \leq x \leq 1.6$,) and bixbyite (Ga,Sn-doped In_2O_3) phases, in the Ga_2O_3-In_2O_3-SnO_2 (GITO) ternary system (**Fig. 1**) have been studied. Although originally discovered at Northwestern in 90s, the scheelite GITO phase was

reported as having only modest conductivity. The Mason group has had recent success in achieving conductivities approaching 1500 S/cm in bulk form. Even higher conductivities (on the order of 4000 S/cm) have been obtained in bulk specimens of Ga,Sn co-doped bixbyite GITO. Combined with band gaps of ~3.1 eV, both phases have strong potential as TCOs. The scheelite GITO phase is of particular interest owing to its relatively lower indium content and the presence of multiple cation sites in the crystal structure (**Fig. 2**). Band structure calculations by the Freeman group display a highly dispersed conduction band minimum (**Fig. 3**), consistent with low effective mass (and high carrier mobility).

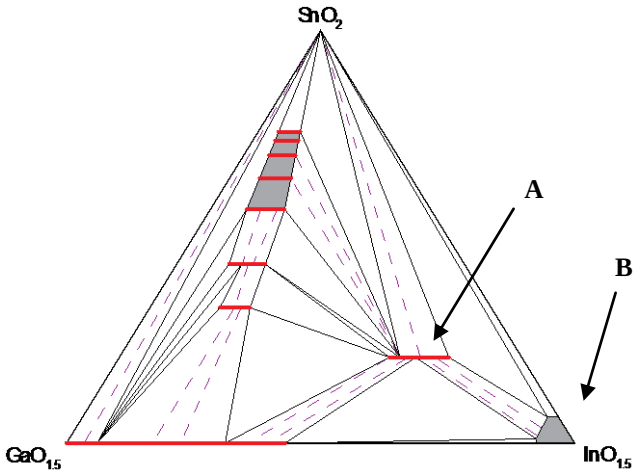

Figure 1. GITO ternary phase diagram, showing the scheelite (A) and bixbyite (B) phases.

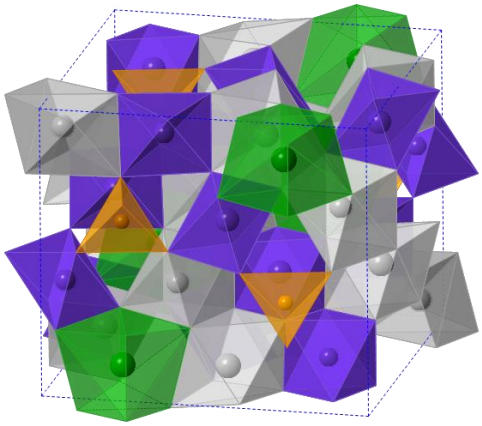

Figure 2. Illustration of the scheelite GITO structure, showing the presence of 4-fold (orange), 6-fold (purple), 7-fold (gray), and 8-fold (green) cation coordination sites.

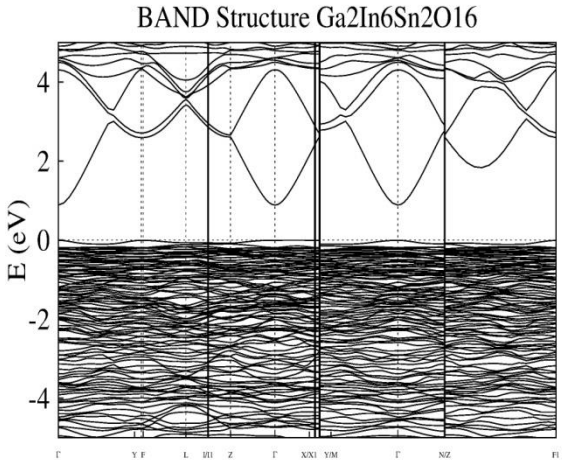

Figure 3. DFT calculation of the band structure of Ga2In6Sn2O16 Scheelite phase using the GGA exchange correlation potential with ion relaxation, showing evidence of the highly dispersed conduction band.

Consistent with our goal of reducing the indium content in TCOs, the Poeppelmeier group has studied the formation of $InTaO_4$. Reaction of the GITO scheelite phase with $Mn_3Ta_2O_8$ (another scheelite phase previously reported in the literature) resulted in two major phases: $InTaO_4$ and a new tetragonal phase (most likely Scheelite). This new driving force provides a route to substitute a large variety cations for the indium present in the Scheelite phase and opens the potential for doping (not just substitution) of Scheelite TCOs.

Building on our prior success with the development of crystalline ZITO (Zn-In-Sn-O) as a lower cost alternative to ITO, high quality crystalline films of $In_{1.4}Sn_{0.3}Zn_{0.3}O_3$, in which 30% of the indium is replaced by cosubstitution (ZITO-30) have been grown in the Chang group by pulsed laser deposition (PLD). These films typically have conductivities of ~2500 S/cm with carrier mobilities of 40 $cm^2/V•s$ but require deposition temperatures above 600°C, making the process incompatible with substrates, such as plastics, that cannot tolerate the higher growth-temperatures. Crystalline films grown at lower temperatures typically have poorer electrical transport properties, in particular lower carrier mobilities. However, determining the effects of growth temperature on the physical structure will give an insight into the optimization of the electrical properties of low growth-temperature films. The most promising materials will be examined in OPVs in collaboration with Marks and Chang.

An initial set of studies was begun to investigate the effect of growth temperature on both the electrical transport properties and optical properties of bixbyite ZITO. Although pure indium oxide is not the end focus of this study, and is rarely used in technological applications, it is the progenitor of many TCO systems, including ZITO, which share the bixbyite structure. Pure indium oxide (IO) has an advantage over doped systems as it removes the ambiguity and convolution introduced by dopants in analyzing experimental results. Therefore, 350 nm thick IO films were grown on fused silica substrates in an initial study that uses IO as the representative bixbyite materials system. As expected, the carrier mobility decreases from ~70 $cm^2/V•s$ to ~20 $cm^2/V•s$ as the growth temperate is decreased from 600°C to 100°C. Commensurate with the decrease in mobility is a degradation in the crystal structure as evidenced by broader and less intense diffraction peaks in the x-ray spectra. Also observed in

this temperature range is a decrease in grain size from ~220 nm to ~100 nm and an increase in lattice constant from ~10.05 Å to ~10.3 Å. Surprisingly, as the temperature is decreased further, from 100°C to 25°C, the carrier mobility does not decrease further but increases from ~20 $cm^2/V•s$ to ~50 $cm^2/V•s$, despite the fact that the X-ray diffraction peaks progressively lose intensity and broaden; the grain size continues to decrease to ~50 nm and the lattice constant increases to ~10.35 Å. Studies are planned to use EXAFS at the Advanced Photon Source (at nearby Argonne National Lab) to determine the In-O coordination number, the In-O bond distance and In-In bond distance as a function of deposition temperature to obtain a better picture of this high-performance low-crystallinity state.

The Chang group has also developed a process to synthesize 3-D TCO nanowire-arrays as electrode structures. In particular, they successfully fabricated lithographically-patterned ITO nanowire arrays with varying heights (up to 15 microns) and spacings as close as 400 nm. Using these wires, they were able to fabricate solar cells with 3D geometry. Preliminary experiments have indicated that cell efficiency can be improved by as much as 30% for the case of dye sensitized solar cells (DSSC). This is due to improved charge collection and transport within the cell, and will next be applied to OPVs in collaboration with Marks.

High efficiency bulk hetero-junction organic photovoltaic (OPV) cells require selective transport and collection of specific charge carriers (holes or electrons) without significant recombination at the charge selection layer. To date, several groups have reported various materials for electron- or hole-selective electrode interfacial layers. Note that the heavily used ITO/PEDOT:PSS/Active Layer/LiF/Al-based normal cell structure has stability problems owing to the corrosive nature of PEDOT:PSS and the low work function of Al. Inversion of the cell structure and using an inorganic interfacial layer (IFL) significantly improves device stability and power conversion efficiency (PCE). For the hole-selective electrode, high electron affinity transition metal oxides (TMO), such as MoO_3 and WO_3, appear to be efficient recombination layers with holes in donor polymers and electrons in transition metal oxides. Unfortunately, stable electron-selective layers are not generally available at this moment. Although some high efficiency OPV cells have been made with n-type semiconductors such as nanocrystalline-ZnO, a-ZnO, a-TiO_x (a=amorphous) and cross-linked fullerene derivatives, execution of this general design concept requires further materials development. Furthermore, recent works have focused only on electron selection from the fullerene derivative in the active layer.

The Marks group has demonstrated for the first time that the conduction band minimum (CBM) of transparent post-transition metal oxide semiconductors can be specifically tuned for various acceptors in OPV active layers. From the Periodic Table, simple binary oxides in group 12 to 15 provide a wide range of CBMs and wide band gaps. The CBMs of these oxides range from very deep-lying heavy metals (Period 6) to low-lying light metals (Period 3). Even further, the mixed amorphous oxide materials show excellent electron transport, unlike conventional a-Si, and chalcogenide glasses. The bond angle distortion-induced trap states are minimized with the spherical nature of s-orbital-based conduction band. Also dangling bonds do not exist in amorphous metal oxide semiconductors due to the ionic nature of metal-oxygen bonding. As shown in **Fig. 4a**, if the low lying heavy metal cation (In) s-orbital and high lying light metal cation(Ga) s-orbtial are mixed homogenously, the continuous alloying of the two extreme CBM positions could provide intermediate/tunable CBM values. We find that the continuous tuning of CBM with amorphous $In_{2-x}Ga_2O_3$ (a-IGO) is possible using combustion synthesis techniques. Since the VBM of ionic metal oxide semiconductors from localized oxygen 2p orbitals is

relatively constant, optical band gap measurements can the reveal relative positions of the CBMs. Thus, optical measurements on a-IGO (**Fig. 4b**) show continuous tuning of the CBM position. The dependence of OPV performance on the electron-transporting IFL CBM value was subsequently confirmed using inverted solar cells having an ITO/a-IGO/PTB7:PC71BM/MoO_3/Ag structure (**Fig. 5**). Note that the low-lying high In content sample gives low a fill factor and V_{oc}, and once the CBM of a-IGO rises above the PC71BM LUMO level, significant OPV performance degradation is observed. However, the maximum OPV performance is achieved with 60-70% Ga contents. The properly aligned CBM and deep lying VBM of post-transition metal oxide semiconductors enable high efficiency inverted OPV cells with a PCE over 8.0%. IFL energy level measurements are currently in progress using IETS spectroscopy with Professor M. Yoshida of Kyoto U., as is band structure computation in collaboration with Freeman.

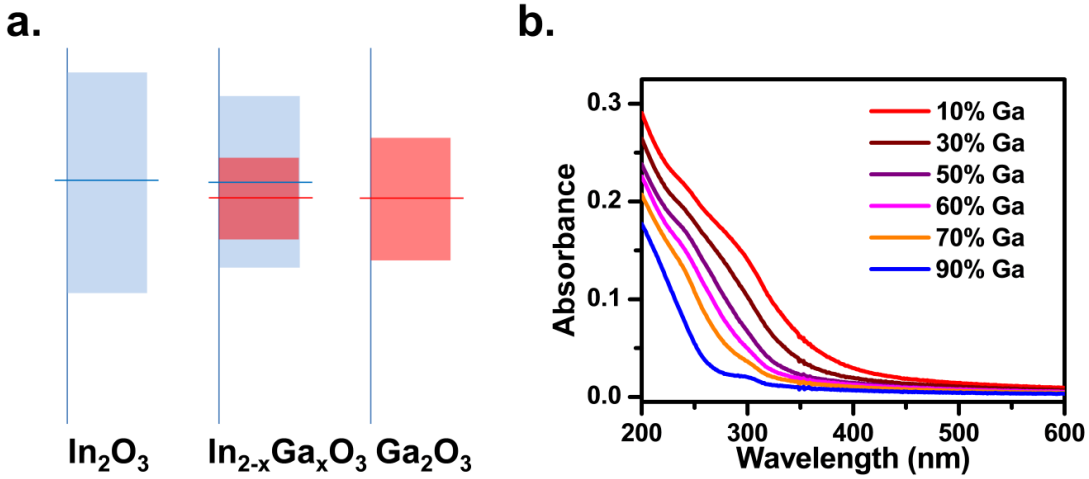

Figure 4. (**a**) Schematic representation of conduction band minimum position tuning. (**b**) Optical spectra of a-IGO.

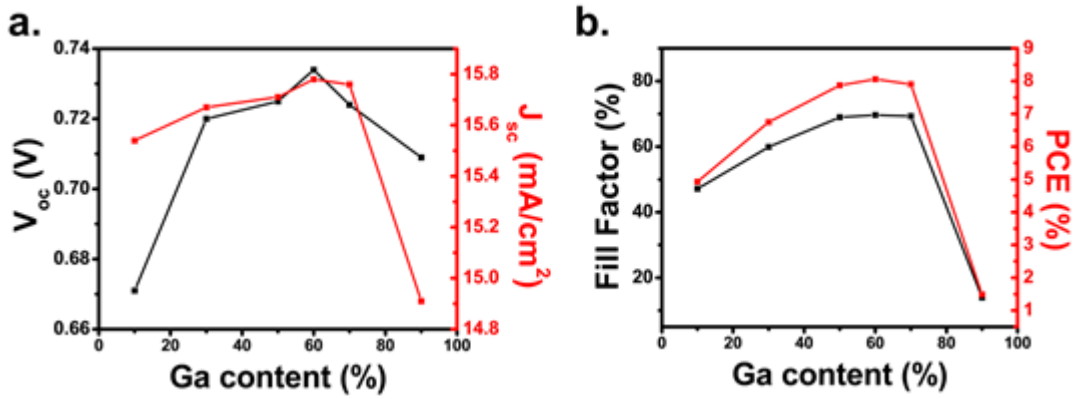

Figure 5. Bulk hetero junction organic photovoltaic cell performance dependence on Ga content in a-IGO interfacial layer. (**a**) Open circuit voltage (V_{oc}) and short circuit current (J_{sc}) dependence. (**b**) Fill factor and power conversion efficiency (PCE) dependence.

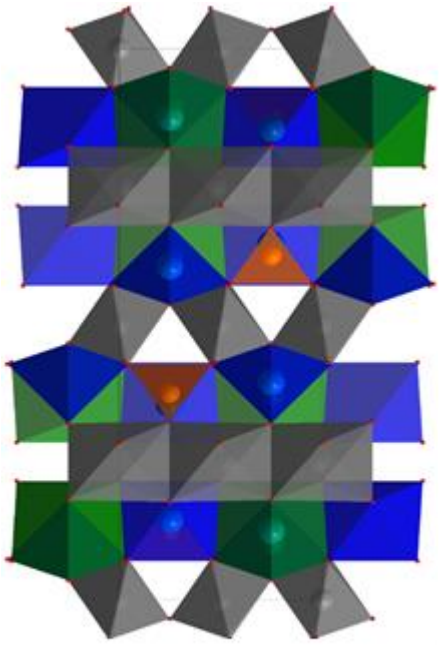

Figure 6. The ZIGO structure, depicting the b-site analogues (gray), 4-coordinate (orange), 6-coordinate In (blue), and 8-coordinate (green) cation environments.

As noted above, the research goals of this five-PI effort were: 1) Theory-guided design and synthesis of advanced TCO/TCM layers with high conductivity and transparency, with work function tunability, and with minimal or no In. 2) Developing theory-based understanding of ideal interfaces between oxide electrodes/interfacial layers and OPV organic active layers composed of molecules or polymers. 3) Exploring and developing new processing techniques and cell architectures for next-generation large-area flexible OPVs. It is our plan that results from our research will continue to lead the way and support other DOE-funded energy programs. Significant progress was made in each of the above areas as outlined below.

A. ***Advanced TCOs*****.** The objectives of this research path were twofold, to synthesize novel materials with potential TCO properties and to enhance the TCO properties of existing materials. The former was accomplished by Poeppelmeier in the investigation of the ZnO-In_2O_3-GeO_2 phase space. Unlike similar systems, a bixbyite solid solution with In_2O_3 as the dominant component does not appear to exist for appreciable amounts of ZnO and GeO_2. Instead, Poeppelmeier discovered a single defined compound, $Zn_{0.456}In_{1.084}Ge_{0.460}O_3$ (ZIGO). Notably, ZIGO has a reduced In content (54 mol %) and conductivity and transparency values that are comparable to that of In_2O_3. Furthermore, the ZIGO structure (**Fig. 6**) contains twice as many cation coordination sites that are equivalent to the b-site of In_2O_3, which is the preferred location for Sn doping to form ITO. Thus ZIGO is particularly interesting as a host for future dopant studies to produce competitive TCOs.

The Ga_2O_3-In_2O_3-SnO_2 (GITO) ternary T-phase, $Ga_{3-x}In_{5+x}Sn_2O_{16}$ ($0.3 \leq x \leq 1.6$) was the focus of the second objective and was studied in a three-way Mason, Poeppelmeier, and Freeman collaboration. Although only moderate conductivity was reported at the time of its discovery at Northwestern, recent developments show that the conductivity can be optimized by manipulating sample composition and processing, yielding values near 2000 S/cm in bulk

specimens. Local density approximation calculations by Freeman and combined conductivity and thermopower measurements by Mason indicate that the carrier mobility and Fermi level are essentially invariant with sample composition and processing conditions. This phenomenon was investigated with first-principles theory using Freeman's full-potential linearized augmented plane wave (FLAPW) technique and the Vienna Ab-initio Simulation

Package and experimental characterization using Mason's optical band gap determination techniques. The invariance across compositions is attributed to two offsetting factors—a decreasing fundamental band gap as a function of x (**Fig. 7**) and a corresponding increase in carrier content (and Burstein-Moss shift) at higher In levels. The predictions were experimentally corroborated, with theory predicting a 2.60 eV fundamental band gap for the x = 1.0 $Ga_{3-x}In_{5+x}Sn_2O_{16}$ and experiments measuring a 2.9 eV optical band gap. Furthermore, the effective carrier masses are essentially invariant at ~0.2 m_e in all directions and do not change with composition (**Table I**).

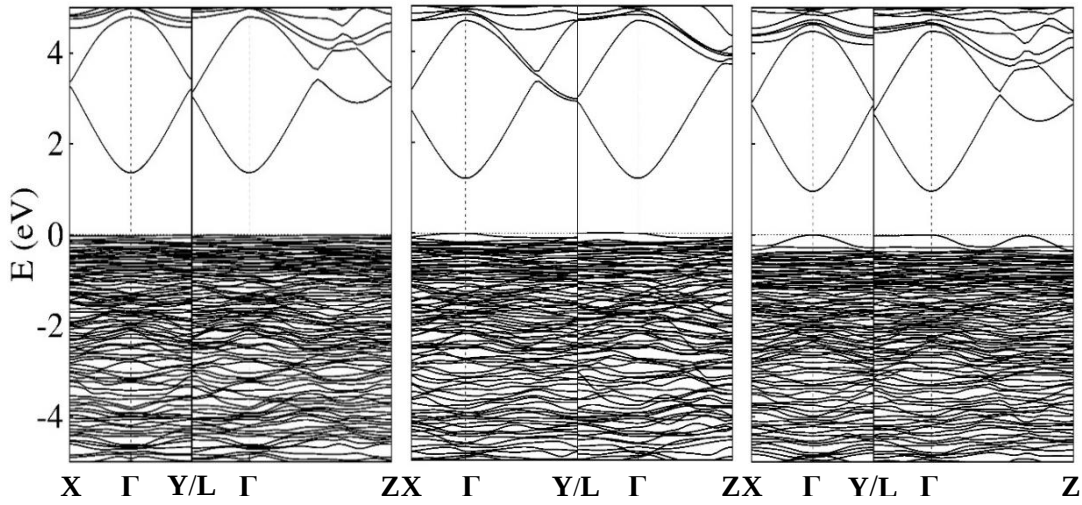

Figure 7. T-phase GITO ($Ga_{3-x}In_{5+x}Sn_2O_{16}$) band structure as a function of composition. Left to right: x = 0.5, x = 1.0, and x = 1.5; LDA-calculated fundamental band gaps are 1.36, 1.21, and 0.96 eV, respectively.

Table I. Effective computed mass for various GITO ($Ga_{3-x}In_{5+x}Sn_2O_{16}$) compositions

	Effective Mass (m^*/m_e)		
Direction	***x = 0.5***	***x = 1.0***	***x = 1.5***
[100]	0.19	0.18	0.18
[010]	0.19	0.18	0.18
[001]	0.21	0.19	0.19

The bixbyite (Ga,Sn-doped In_2O_3) phase in the GITO system was also studied. A two-variable regression analysis of the bixbyite lattice parameter was used to determine the phase boundaries of the GITO bixbyite phase and its equilibria with tin oxide, β-gallia, and T-phase GITO (**Fig. 8**). Furthermore, the impact of Ga and Sn content was assessed. As anticipated, the conductivity is heavily dependent on the amount of Sn doped into the material. Alternative Ga contents, however, did not appear to have a notable effect on the TCO properties of the resulting material. Thus Ga was deemed to act as an isovalent dopant.

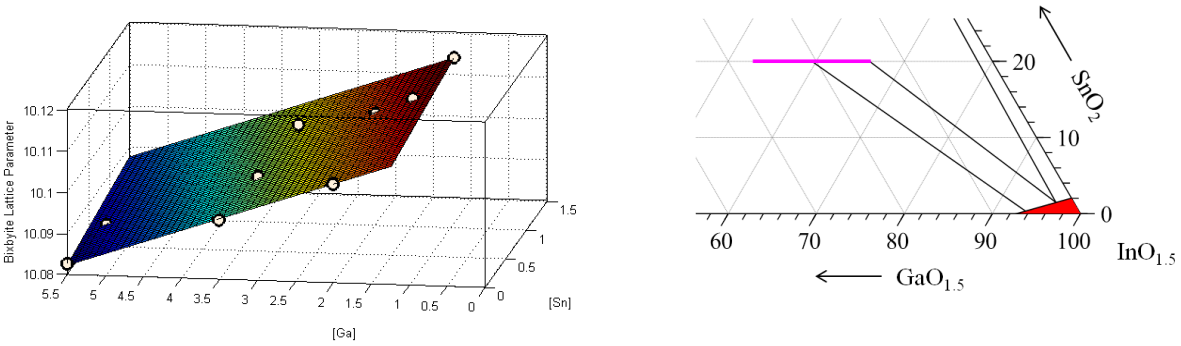

Figure 8. (Left) There-dimensional representation of the two-variable linear regression of the GITO bixbyite lattice parameter (in Å) with substitution of In by Ga and Sn (R^2_{adj} = 0.9952). [Ga] and [Sn] are plotted in atomic %. (Right) Select phases in the In_2O_3corner of the GITO phase diagram at 1250 °C, showing the refined bixbyite (red) phase boundaries and its equilibria with the T-phase (pink) and SnO_2.

Single crystals of high temperature phases of Ga- and/or In-containing materials are difficult to obtain as a result of the volatility of Ga and In. Although crystal growth investigations are underway for GITO, isostructural materials exist that are more readily grown as single crystals. Poeppelmeier has successfully grown one of these materials, $Mn_3Ta_2O_8$, and characterized it both experimentally and computationally. This material, being isostructural to GITO, has 4 different cation coordination environments: 4-, 6-, 7-, and 8-coordinate. Although the occupancies of these sites is complex in GITO, they are simplified by the fewer elements present

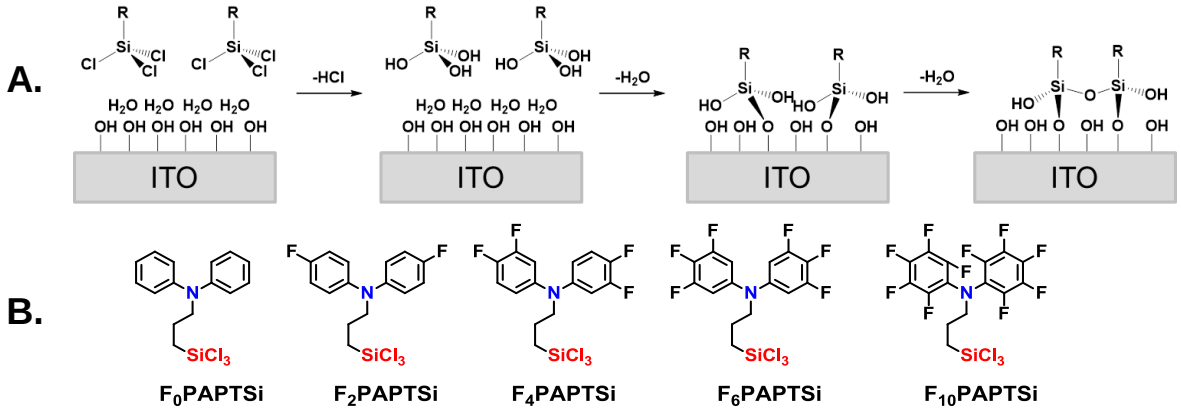

Figure 9. A. Schematic of organosilane chemisorption onto ITO surfaces. $SiCl_3$ moieties first hydrolyze, then condense with surface –OH groups and crosslink to form dense, robust, electroactive films. **B**. Interfacial layer (IFL) precursor series examined in this study.

in $Mn_3Ta_2O_8$ and the greater differences inherent in these elements. Thus a major finding of the $Mn_3Ta_2O_8$ investigation, that the electronic transition over the band gap is governed only by the 4- and 7- coordinate sites, may be able to be extended to GITO. If such an extension is possible, then the optical properties of GITO can be further optimized.

B. Probing Interfacial Layer Function. To better understand and enhance anode performance in bulk-heterojunction (BHJ) OPVs, Marks modified the anode ITO/active layer interface with a series of robust silane-tethered bis(fluoroaryl)amines, designed with the guidance of DFT calculations, to offer large excursions in the molecular dipole moment, and to form self-assembled interfacial layers (IFLs) as shown in **Fig 9** These layers are stable to very high temperatures, impervious to most organic and inorganic solvents, and pass the ASTM "Scotch tape" mechanical adhesion test. The modified ITO anodes were characterized by advancing aqueous and hydrocarbon contact angle measurements, X-ray reflectivity (XRR), ultraviolet photoelectron spectroscopy (UPS), X-ray photoelectron spectroscopy (XPS), grazing incidence X-ray diffraction (GIXRD), AFM, and solution phase cyclic voltammetry. These techniques reveal the presence of hydrophobic, densely packed amorphous monolayers of 6.68 to 9.76 Å thickness, and having modified anode work functions ranging from 4.66 to 5.27 eV.

Two series of glass/ITO/IFL/active layer/LiF/Al BHJ OPVs were fabricated with the active layer = poly(3-hexylthiophene):phenyl-C_{71}-butyric acid methyl ester (**P3HT:PC$_{71}$BM**) or poly[[4,8-bis[(2-ethylhexyl)oxy]benzo[1,2-b:4,5-b']dithiophene-2,6-diyl][3-fluoro-2-[(2-ethylhexyl)-carbonyl]thi-eno[3,4-b]thiophenediyl]]:phenyl-C_{71}-butyric acid methyl ester (**PTB7:PC$_{71}$BM**). OPV analysis under AM 1.5G conditions reveals significant performance enhancement versus unmodified glass/ITO anodes. Strong positive correlations between the electrochemically-derived heterogeneous electron transport rate constants (k_s) and the device open circuit voltage (V_{oc}),short circuit current (J_{sc}), hence OPV power conversion efficiency (PCE), are observed for these modified anodes. Furthermore, the strong functional dependence of the device metrics on k_s increases as greater densities of charge carriers are generated in the BHJ OPV active layer, and is attributable to enhanced anode carrier extraction in the case of high-k_s IFLs.OPVs fabricated with these SAM-modified anodes exhibit V_{oc}, J_{sc} and therefore PCE metrics that most closely track the *cyclic voltammetry-derived heterogeneous electron transport rate constants*, k_ss. Furthermore, these experiments show for the first time that k_s scales as the SAM out-of-plane dipole moment and surface coverage, which enhance hole extraction and suppress recombination processes. In the coming grant period the team will explore new ways to enhance IFL packing and the consequences thereof, especially on non-ITO surfaces such as Poeppelmeier's GITO, the nanostructured ITOs of Chang's dye-sensitized solar cells (DSSCs), amorphous ZITO (see below), and explore the properties of tunable work function inorganic IFLs.

C. Crystalline to Amorphous InO_x Transition. Chang, in collaboration with Mason and Qin Ma of the Argonne APS, has studied the pure indium oxide, a progenitor of many TCO systems, including ZITO and GITO. Pure indium oxide (IO_x) has an advantage over doped systems as it removes the ambiguity and convolution introduced by dopants in analyzing experimental results, particularly in interpreting EXAFS data. Therefore, Chang focused on IO_x films during the past year. Data gathered from these studies has helped other team members to better understand their complex oxide systems. IO_x films (typically 350 nm thick) were grown on fused silica

substrates in an initial study using IO_x as the representative bixbyite materials system. As expected, the carrier mobility falls from ~70 $cm^2/V•s$ to ~20 $cm^2/V•s$ as the growth temperate is decreased from 600°C to 100°C. Commensurate with the decreased mobility is degradation in the crystal structure evident in X-ray diffraction measurements, with reduction in the grain size from ~220 nm to ~100 nm and an increase in the lattice constant from ~10.05 Å to ~10.3 Å. Only minor changes in the local structure are evident by EXAFS on cooling. Thus, in the first-shell, the In-O coordination number (N_{In-O}) ~6, and the In-O bond distance (R_{In-O}) ~2.17 Å. In the second shell, the In-In coordination number (N_{In-In}) ~6 and the In-In bond distance (R_{In-In}) ~3.36 Å also change little. There is, however a noticeable increase in the statistical spreads of the In-O and In··In bond distances (σ^2_{In-O} and σ^2_{In-In}) from 0.007 $Å^2$ to 0.008 $Å^2$ and from 0.004 $Å^2$ to 0.008 $Å^2$, respectively, and indicating greater disorder in the regular structure. When the deposition temperature is further decreased, from 100°C to 25°C, the carrier mobility does not decrease, but remarkably *increases* from ~20 $cm^2/V•s$ to ~50 $cm^2/V•s$, despite the fact that the X-ray diffraction peaks progressively lose intensity and broaden,, while the grain size continues to decrease to ~50 nm and the lattice constant increases to ~10.35 Å. In this region N_{In-O} falls from ~6 to ~5.3, R_{In-O} falls from 2.17 Å to ~2.14 Å, σ^2_{In-O} remains at ~0.008 $Å^2$, N_{In-In} decreases from ~6 to ~3.8, R_{In-In} remains at ~3.36 Å and σ^2_{In-In} increases from ~0.008 $Å^2$ to ~0.013 $Å^2$. As the fully amorphous region is approached (0ºC), no major changes in N_{In-O}, R_{In-O}, σ^2_{In-O}, R_{In-In} or $\sigma^2_{In-In}$are observed while N_{In-In} decreases to ~2, and the mobility remains high (~50 $cm^2/V•s$). These intriguing results suggest only minor structural changes versus the slightly crystalline films grown at 25°C. As the deposition temperature is decreased even further to -100°C, the mobility decreases to ~20 $cm^2/V•s$. While there are no changes in the EXAFS parameters, x-ray reflectivity of 65 nm thick IO_x films indicates that the film density decreases as the deposition temperature is lowered below the point where x-ray diffraction indicates amorphous films. Better understanding the bulk and surface properties of amorphous TCOs is of both fundamental scientific and ultimate technological interest, and will be pursued in future work.

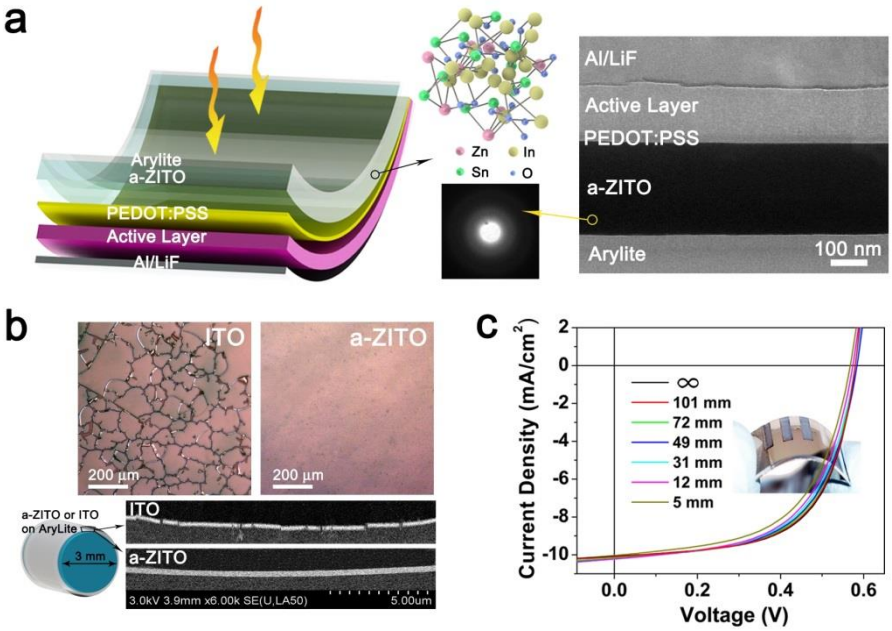

Figure 10. Flexible device architecture, bending properties of a-ZITO and flexible OPVs. **a.** Schematic and cross-sectional TEM image of AryLite/a-ZITO/PEDOT:PSS/Active Layer/LiF/Al device architecture. The EF-SAED pattern of a-ZITO layer shows complete amorphous characteristics. **b.** Optical microscopic and SEM cross-sectional images of

polycrystalline ITO/AryLite and a-ZITO/AryLite substrate, collected after bending at a radius of 5 mm and ~1.5 mm, respectively. **c.** dependence of P3HT:PC_{61}BM and PTB7:PC_{71}BM PSC performance on bending radius, inset showing a fully fabricated flexible OPV.

D. Flexible Solar Cells with Amorphous ZITO Electrodes. Our team fabricated the first a-ZITO films on a plastic foils exhibiting low sheet resistance, high optical transparency, and *mechanical flexibility* for polymer OPV electrodes. These films afford comparable optical and electrical parameters to commercial polycrystalline ITO/glass, and BHJ OPVs were fabricated with two representative donor polymers, **P3HT** and **PTB7** (**Fig. 10**). Compared to ITO-based devices, the a-ZITO/glass and a-ZITO/AryLite^R devices exhibit similar performance metrics, yielding flexible devices with *PCE*s of 3.63% for **P3HT:PC_{61}BM**, and a record high *PCE* of 6.42% for **PTB7:PC_{71}BM**. Bending measurements on both a-ZITO/AryLite substrates and completed OPVs indicate that the substrates retain low sheet resistance <30 Ω/□, and the flexible OPVs retain up to ~90% and ~85%, respectively, of the original *PCE*s after 10x flexing/relaxing at bending radii of ~5 mm. Under the same conditions, ITO/AryLite^R films crack and the OPVs fail. This work demonstrates that a-ZITO electrodes can replace widely used, more In-rich polycrystalline ITO, but can add mechanical flexibility characteristics essential for next-generation ultra-flexible OPVs. The underlying science will be pursued both experimentally and theoretically in the coming project period.

E. 3-D Anodes for DSSCs. During the past year, Chang has perfected the growth of ITO nano-rods to create 3-D solar cell electrodes. His group fabricated dye sensitized solar cells (DSSCs) with these electrodes and showed that the cell efficiency can be increased by ≥15-20% versus conventional 2-D cells. **Fig.11a** shows the cell architecture in 3-D and **Fig.11b** compares the J-V curves of 2-D and 3-D DSSCs as a function of active layer thicknesses. To better understand the increased cell PCE, a finite element simulation was carried out comparing the 2D and 3D geometries. The simulation verifies our concept that 3D geometries have reduced internal resistance for electrons traveling to the external circuit, especially for 450 - 650 nm light where longer pathlengths are required for N719 dye light absorption. This 3-D architecture strategy should be applicable to other types of solar cells, and will be explored in future work, as will the consequences of implementing Marks' self-assembling organosilane IFLs (Section B) to DSSCs.

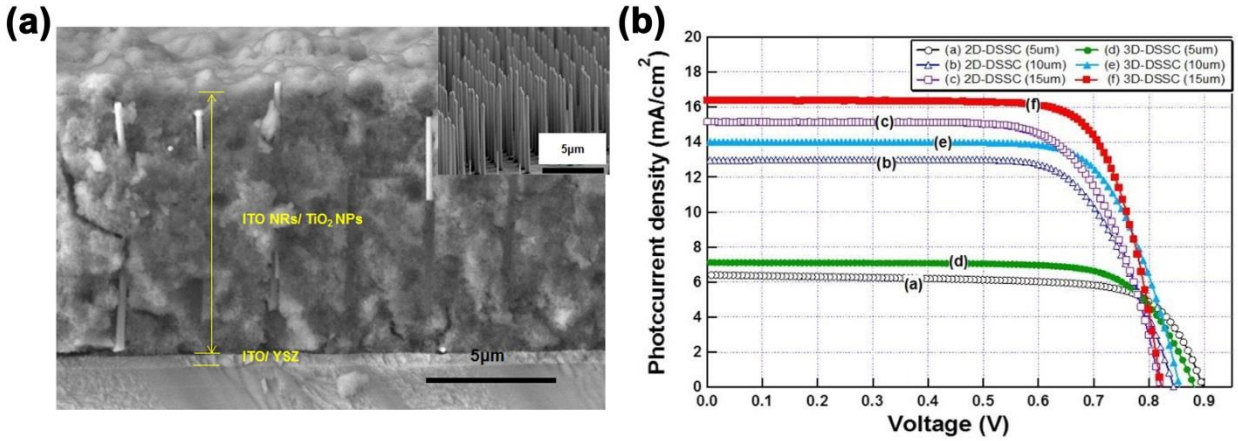

Figure 11. **a**. SEM image of a 3-D DSSC with active materials filled among the ITO nano-rods. The in-set shows as grown nano-rods. **b.** a comparison of J-V curves of 2-D cells versus 3-D cells for different active layer thicknesses.

Publications During the Project Period Acknowledging Grant ER46536

Stampler, E. S.; Sheets, W. C.; Bertoni, M. I.; Prellier, W.; Mason, T. O.; Poeppelmeier, K. R.; Temperature Driven Reactant Solubilization Synthesis of BiCuOSe, *Inorg. Chem*., **2008**, 47, 10009.

Hains, A.W.; Marks, T.J., High-Efficiency Hole Extraction/Electron-Blocking Layer to Replace Poly (3,4-ethylenedioxythiophene):Poly (styrene sulfonate) (PEDOT:PSS) in Bulk-Heterojunction Polymer Solar Cells, *Appl. Phys. Lett*., **2008**, 92, 023504.

Irwin, M. D.; Buchholz, D. B.; Hanis, A. W.; Chang, R. P. H.; Marks, T. J.; p-Type semiconducting nickel oxide as an efficiency-enhancing anode interfacial layer in polymer bulk-heterojunction solar cells, *Proc. Natl. Acad. Sci*., **2008**, 105, 2783.

Harvey, S. P.; Mason, T. O.; Körber, C.; Klein, A.; Bulk Defect Chemistry and Surface Electronic Behavior of Zn,Sn Codoped In2O3 Transparent Conducting Oxides, *Phys. Chem.*, **2009**, 11, 3099.

Proffit, D. E.; Buchholz, D. B.; Chang, R. P. H.; Bedzyk, M. J.; Mason, T. O.; Ma, Q.; X-Ray Absorption Spectroscopy Study of the Local Structures of Crystalline Zn–In–Sn Oxide Thin Films, *J. Appl. Phys*., **2009**, 106 (11), 113524:1-6.

Klein, A.; Körber, C.; Wachau, A.; Säuberlich, F.; Gassenbauer, Y.; Schafranek, R., Harvey, S. P.; Mason, T. O.; Surface Potentials of Magnetron Sputtered Transparent Conducting Oxides, *Thin Solid Films*, **2009**, 518 (4), 1197-1203

Buchholz, D. B.; Liu, J.; Marks, T. J.; Zhang, M.; Chang, R. P. H.; Control and Characterization of the Structural, Electrical, and Optical Properties of Amorphous Zinc−Indium−Tin Oxide Thin Films, A*CS Appl. Mater. Interf.*, **2009**, 1 (10), 2147-2153.

Stampler, E. S.; Sheets, W. C.; Prellier, W.; Marks, T. J.; Poeppelmeier, K. R.; Hydrothermal Synthesis of LnMnO3 (Ln=Ho-Lu and Y): Exploiting Amphoterism in Late Rare-Earth Oxides, *J. Mater. Chem*., **2009**, 19, 4375-4381.

Marrocchi, A.; Silvestri, F.; Seri, F. M.; Facchetti, A.; Taticchi, A.; Marks, T. J.; Conjugated Anthracene Derivatives as Donor Materials for Bulk-Heterojunction Solar Cells: Olefinic versus Acetylenic Spacers, *Chem. Commun.*, **2009**, 1380-1382.

Liu, J.; Hains, A.; Servaites, J.; Ratner, M.; Marks, T.J.; Highly Conductive Bilayer Transparent Conducting Oxide Thin Films for Large-Area Organic Photovoltaic Cells, *Chemistry of Materials*, **2009**, 21, 5258.

Irwin, M. D.; Buchholz, D. B.; Leever, B. J.; Liu, J.; Emery, J. D.; Zhang, M.; Song, J.-H.; Durstock, M. F.; Freeman, A. J.; Bedzyk, M. J; Hersam, M. C.; Chang, R. P. H.; Marks, T. J.; Microstructure, Electronic Structure, and Function of NiO Anode Overlayers in High-Efficiency P3HT:PCBM Bulk-Heterojunction Organic Photovoltaic Devices, *J. Am. Chem. Soc.*, **2010**, submitted.

Hains, A. W.; Martinson, A. B. F.; Liu, J.; Irwin, M. D.; Marks, T. J.; Anode Interfacial Tuning via Electron-Blocking/Hole-Transport Layers and Indium Tin Oxide Surface Treatment in Bulk-Heterojunction Photovoltaic Cells, *Adv. Funct. Mater*., **2010**, 20, 595-606.

Mansourian-Hadavi, N.; Wansom, D.; Mason, T. O.; Ye, L.; Freeman, A. J.; Transport and Band Structure Studies of Crystalline ZnRh2O4, submitted to *Phys. Rev. B*.. **2010**, 81, 075112.

Hains, A. W.; Ramanan, C.; Irwin, M. D.; Liu, J.; Wasielewski, M. R.; Marks, T. J.; Designed Bithiophene-Based Interfacial layer for High-Efficiency Bulk-Heterojunction Organic Photovoltaic Cells. Importance of Interfacial Energy Level Matching, *ACS Appl. Mater. Interf*., **2010**, 2, 175-185.

Hoel, C. A.; Mason, T. O.; Gaillard, J.-F.; Poeppelmeier, K. R.; Transparent Conducting Oxides in the ZnO-In2O3-SnO2 System, *Chemistry of Materials*, **2010**, 22 (12), 3569.

Peng, H.; Song, J.-H.; Hopper, E. M.; Zhu, Q.; Mason, T. O.; Freeman, A. J.; Possible n–type carrier sources in In2O3(ZnO)k, *Chemistry of Materials*, **2011**, 24 (1), 106.

Irwin, M.D.; Servaites, J.D.; Buchholz, D.B.; Leever, B.J.; Liu, J.; Emery, J.D.; Zhang, M.; Song, J.-H.; Durstock, M.F.; Freeman, A.J.; Bedzyk, M.J.; Hersam, M.C.; Chang, R.P.H.; Ratner, M.A.; Marks, T.J.; Structural and Electrical Functionality of NiO Interfacial Films in Bulk Heterojunction Organic Solar Cells, *Chem. Mater*., **2011**, 23, 2218–2226.

Peng, H.; Song, J.-H.; Hopper, E. M.; Zhu, Q.; Mason, T. O.; Freeman, A. J.; Possible n-type carrier sources in In2O3(ZnO)(k), *Chemistry of Materials*, **2012**, 24, 106.

Hopper, E. M.; Sauvage, F.; Chandiran, A. K.; Grätzel, M.; Poeppelmeier, K. R.; Mason, T. O.; Electrical Properties of Nb-, Ga-, and Y-Substituted Nanocrystalline Anatase TiO2 Prepared by Hydrothermal Synthesis, *Journal of the American Ceramic Society*, **2012**, 95 (10), 3192-3196.

Buchholz, D. B.; Proffit, D. E.; Wisser, M. D.; Mason, T. O.; Chang, R. P. H.; Electrical and band-gap properties of amorphous zinc–indium–tin oxide thin films, *Progress in Natural Science: Materials International*, **2012**, 22 (1), 1-6.

Hoel, C. A.; Buchholz, D. B.; Chang, R. P. H.; Poeppelmeier, K. R.; Pulsed-laser deposition of heteroepitaxial corundum-type ZITO: cor-In-2 (-) (2x) ZnxSnxO3, *Thin Solid Films*, **2012**, 520, 2938-2942.

Lee, B.; Buchholz, D. B.; Chang, R. P. H.; An all carbon counter electrode for dye sensitized solar cells, *Energy & Environmental Science*, **2012**, 5 (5), 6941-6952.

Hopper, E.M.; Peng, H.; Hawks, S. A.; Freeman, A. J.; Mason, T. O.; Defect mechanisms in the In2O3(ZnO)k system (k = 3, 5, 7, 9), *Journal of Applied Physics*, **2012**, 112, 093712.

Yoon, S. M.; Lou, S. J.; Loser, S.; Song, C. K.; Je, J. H.; Smith, J. A.; Chen, L. X.; Facchetti, A.; Marks, T. J.; Fluorinated Copper Phthalocyanine Nanowires for Enhancing Interfacial Electron Transport in Organic Solar Cells, *Nano Letters* **2012**, 12, 6315-6321.

Hopper, E. M.; Zhu, Q.; Gassmann, J.; Klein, A.; Mason, T. O.; Surface electronic properties of polycrystalline bulk and thin film In2O3(ZnO)k compounds, *Applied Surface Science*, **2013**, 264 (0), 811.

Buchholz, D. B.; Zeng, L.; Bedzyk, M. J.; Chang, R. P. H.; Differences between amorphous indium oxide thin films, *Progress in Natural Science: Materials International* **2013**, 23, 475-480.

Song, C. K.; White, A. C.; Zeng, L.; Leever, B. J.; Clark, M. D.; Emery, J. D.; Lou, S. J.; Timalsina, A.; Chen, L. X.; Bedzyk, M. J.; Marks, T. J.; Systematic Investigation of Organic Photovoltaic Cell Charge Injection/Performance Modulation by Dipolar Organosilane Interfacial Layers, *ACS Applied Materials & Interfaces*, **2013**, 5, 9224-9240.

Dolgonos, A.; Lam, K.; Poeppelmeier, K. R.; Freeman, A. J.; Mason, T. O.; Electronic and optical properties of Ga3−xIn5+x Sn2O16: An experimental and theoretical study, *J. Appl. Phys.* **2014**, 115, 013703.

Loser, S.; Valle, B.; Luck, K. A.; Song, C. K.; Ogien, G.; Hersam, M. C.; Singer, K. D.; Marks, T. J.; High-Efficiency Inverted Polymer Photovoltaics via Spectrally Tuned Absorption Enhancement, *Advanced Energy Materials*, **2014**, 4, 1301938.

Zhou, N.; Buchholz, D. B.; Zhu, G.; Yu, X.; Lin, H.; Facchetti, A.; Marks, T. J.; Chang, R. P. H.; Ultraflexible Polymer Solar Cells Using Amorphous Zinc−Indium−Tin Oxide Transparent Electrodes, *Advanced Materials*, **2014**, 26, 1098-1104.

Song, C. K.; Luck, K.A.; Zhou, N.; Zeng, L.; Manley, E.; Heitzer, H.M.; Goldman, S.; Hersam, M.C.; Chang, R.P.H.; Bedzyk, M.J.; Chen, L.X.; Ratner, M.A.; Marks, T.J.; "Supersaturated" Self-Assembled Charge-Blocking Layers for Organic Solar Cells, *J. Amer. Chem. Soc*., **2014**, 136, 17762–17773.

Lee, B; Guo, P; Li, S-Q; Buchholz, D.B.; Chang, R.P.H.; Three Dimensional Indium-Tin-Oxide Nanorod Array for Charge Collection in Dye-Sensitized Solar Cells, *ACS Applied Materials & Interfaces*, **2014**, 6, 17713-17722.

Dolgonos, A.; Wells, S. A.; Poeppelmeier, K. R.; Mason, T. O.; Phase Stability and Optoelectronic Properties of the Bixbyite Phase in the Gallium-Indium-Tin-Oxide System, *J. Am. Ceram. Soc.* **2015**, 98, 669-674.

Kim, M.-G.; Zhou, N. Loser, S.C.; Yoshida H.; Smith J. Guo, X.; Song, C. K.; Jin, H; Yoon S. M.; Freeman, A. J.; Chang, R. P. H.; Facchetti, A.; Marks, T.J.; Amorphous Oxide Interfacial Layers in Inverted Organic Solar Cells. Energy Level Tuning to Match Organic Active Layer Components, *PNAS*, **2015**, 112, 7897-7902.

Rickert, K.; Pozzi, E. A.; Khanal, R.; Onoue, M.; Trimarchi, G.; Medvedeva, J. E.; Hersam, M. C.; Van Duyne, R. P.; Poeppelmeier, K. R.; Selective Crystal Growth and Structural, Optical, and Electronic Studies of Mn3Ta2O8, *Inorg. Chem*., **2015**, 54, 6513-6519.